

Inhibition of Radiation and Temozolomide-Induced Invadopodia Activity in Glioma Cells Using FDA-Approved Drugs



Clarissa A. Whitehead^{*}, Hong P.T. Nguyen^{*}, Andrew P. Morokoff^{*†}, Rodney B. Luwor^{*}, Lucia Paradiso^{*}, Andrew H. Kaye^{*†}, Theo Mantamadiotis^{*‡} and Stanley S. Stylli^{*†}

^{*}Department of Surgery, The University of Melbourne, The Royal Melbourne Hospital, Parkville, Victoria 3050, Australia; [†]Department of Neurosurgery, The Royal Melbourne Hospital, Parkville, Victoria 3050, Australia; [‡]Department of Microbiology & Immunology, School of Biomedical Sciences, The University of Melbourne, Parkville VIC 3010, Victoria, Australia

Abstract

The most common primary central nervous system tumor in adults is the glioblastoma multiforme (GBM). The highly invasive nature of GBM cells is a significant factor resulting in the inevitable tumor recurrence and poor patient prognosis. Tumor cells utilize structures known as invadopodia to facilitate their invasive phenotype. In this study, utilizing an array of techniques, including gelatin matrix degradation assays, we show that GBM cell lines can form functional gelatin matrix degrading invadopodia and secrete matrix metalloproteinase 2 (MMP-2), a known invadopodia-associated matrix-degrading enzyme. Furthermore, these cellular activities were augmented in cells that survived radiotherapy and temozolomide treatment, indicating that surviving cells may possess a more invasive phenotype posttherapy. We performed a screen of FDA-approved agents not previously used for treating GBM patients with the aim of investigating their “anti-invadopodia” and cytotoxic effects in GBM cell lines and identified a number that reduced cell viability, as well as agents which also reduced invadopodia activity. Importantly, two of these, paclitaxel and vinorelbine tartrate, reduced radiation/temozolomide-induced invadopodia activity. Our data demonstrate the value of testing previously approved drugs (repurposing) as potential adjuvant agents for the treatment of GBM patients to reduce invadopodia activity, inhibit GBM cell invasion, and potentially improve patient outcome.

Translational Oncology (2018) 11, 1406–1418

Introduction

Malignant gliomas are among the deadliest and most invasive types of cancer, resulting in serious impairment of quality of life in patients and ultimately mortality. Gliomas account for approximately 80% of all brain-related malignancies [1], with an incidence of 5.26 per 100,000 people in the United States [2], contributing to approximately 2.7% of all cancer-related deaths or over 23,000 new patients expected annually [3]. The most prevalent and aggressive form of glioma, known as glioblastoma multiforme (GBM, WHO Grade IV), accounts for 55% of all gliomas and 15% of all primary and central nervous system tumors [4]. A vital characteristic of all gliomas, and in particular GBM, is that the cells are highly invasive, which allows them to migrate away from the primary tumor and infiltrate the surrounding normal-in-appearance brain parenchyma. This wide-

spread invasion severely limits surgical resection of the tumor, and consequently, following surgical resection, tumor cells remain and the tumor inevitably relapses, with 90% of secondary tumors occurring within 2–3 cm of the original tumor mass [5]. GBM is also considered

Address all correspondence to: Stanley S. Stylli, PhD, Level 5, Clinical Sciences Building, Department of Surgery, The University of Melbourne, The Royal Melbourne Hospital, Parkville, Victoria 3050, Australia. E-mail: stanley.stylli@mh.org.au
Received 18 July 2018; Revised 27 August 2018; Accepted 27 August 2018

© 2018 The Authors. Published by Elsevier Inc. on behalf of Neoplasia Press, Inc. This is an open access article under the CC BY-NC-ND license (<http://creativecommons.org/licenses/by-nc-nd/4.0/>).
1936-5233/18
<https://doi.org/10.1016/j.tranon.2018.08.012>

incurable, with 26.5% of GBM patients surviving 2 years postdiagnosis [6], 5.5% surviving 5 years [2,7], and a median survival rate of just 15 months with the current standard treatment consisting of surgical resection followed by concomitant radiotherapy and chemotherapy with the DNA-alkylating drug temozolomide (TMZ) [8]. Importantly, contributing to the poor outcome of GBM patients is the development of resistance to radiotherapy and TMZ treatment [9].

Research has shown that a key mechanism of GBM cell invasion is facilitated by the formation of dynamic, actin-rich protrusions known as invadopodia [10,11]. These specialized membrane structures are able to reach lengths greater than 2 μm, with diameters ranging from 0.1 to 0.8 μm [11], and function to degrade the surrounding matrix through the action of transmembrane proteases, such as MT1-MMP, and secreted proteases, such as MMP-2 and MMP-9 [12], ultimately facilitating malignant cell invasion through the modified surrounding extracellular matrix (ECM). The presence of invadopodia in glioma cells lines and cells harvested from GBM patient specimens has been previously documented [11,13,14], suggesting that they may potentially play a role in glioma cell invasion. Importantly, we have previously shown that the expression levels of an invadopodia regulator, Tks5, in glioma patient biopsies may be of prognostic significance [15].

The clinical management of many cancers generally involves the use of radiation therapy, with approximately 50% of cancer patients receiving radiation therapy during the course of their disease [16]. Studies have previously reported that radiation therapy can induce an enhancement of MMP-2 secretion in a wide range of cancer cell types, including lung [17], pancreas [18], kidney [19], and glioma [20–22]. This increase in MMP-2 secretion may assist tumor survival by decreasing apoptosis, inducing proliferation and angiogenesis, as well as promoting invasion [23]. GBM cells that receive sublethal doses and survive radiotherapy and/or TMZ treatment have also been shown to exhibit enhanced migratory and invasive potential [24–28], indicating that the long-term inadequacy of treatment observed for most patients may be related to surviving cells exhibiting an increased invasive capacity. This is a crucial aspect as the majority of GBM tumors frequently recur close to initial resection cavity or the target volume of radiotherapy [29]. A previous report by our laboratory has shown that the enhanced invasive phenotype observed in glioma cells posttreatment is possibly mediated by the action of invadopodia [30].

The poor prognosis for many cancers, including GBM, requires the development for new therapies. However, the cost associated with the discovery, development, and registration of a new drug is a significant impediment [31]. As a result, in recent years, drug repurposing (or drug repositioning) has been adopted as a means for identifying new therapeutic applications or indications for already FDA-approved drugs, thereby bypassing the hurdles involved in the discovery and development of new drugs. Importantly, there will already be existing knowledge of toxicities, pharmacokinetics, and dosing for the previous indications, which is not available for newly developed drugs, thereby shortening the developmental time frame of research to clinical use. Also, as these drugs have already been through preclinical pharmaceutical pipelines, the cost of repurposing a drug for a new therapeutic application or indication is significantly reduced [32].

In view of the inherent invasive nature of GBM cells, it may be possible that specifically targeting invadopodia could serve as a novel adjuvant therapeutic strategy in conjunction with the current therapeutic approach. Serendipitously, several drugs have been developed which target factors, including Src, microtubules, and epidermal growth factor receptor (EGFR), which regulate invadopodia-related processes.

Such drugs may be able to impair invadopodia formation and/or activity in GBM. Here, we investigate several FDA-approved agents to examine their therapeutic efficacy and ability to reduce the invasiveness of GBM cell lines by targeting invadopodia activity.

Methods

FDA-Approved Drugs

The FDA-approved drugs utilized in this study were supplied at a concentration of 10 mM in DMSO (Selleckchem) and were stored at –80°C (Table 1).

Cell Lines and Culture

U87MG and LN229 cell lines were purchased from the American Type Culture Collection, while U87MG-EGFRvIII was sourced from the Ludwig Institute for Cancer Research. GBM cell lines MU41 and MU35 were generated from biopsy samples obtained from GBM patients at the time of surgery at The Royal Melbourne Hospital (Melbourne Health Research Ethics Approval Number HREC 2009.116). The cells were cultured in DMEM (Life Technologies) supplemented with 10% (vol/vol) heat-inactivated fetal bovine serum (HyClone), penicillin (100 U/ml), and streptomycin (10 μg/ml). All cells were maintained in a humidified atmosphere of 10% CO₂ at 37°C and used within the first 20 cell passages.

Western Blot Analysis

Western blot analysis of protein lysates (20 μg) was performed using NuPage 4%-12% bis-tris precast gels (Invitrogen) and transferred onto nitrocellulose blotting membrane (GE Healthsciences). The membranes were blocked with 3% bovine serum albumin in 1% TBST for 1 hour prior to overnight incubation with primary antibodies at 4°C. The following antibodies were used: cortactin (diluted 1:1000, Santa Cruz Biotechnology), phosphocortactin (diluted 1:1000, Cell Signaling Technologies), GAPDH (diluted 1:1000, Cell Signaling Technologies), N-WASP (diluted 1:1000, Santa Cruz Biotechnology), Nck1 (diluted 1:1000, Cell Signaling Technologies), MMP-2 (diluted 1:1000, Santa Cruz Biotechnology), Tks5 (diluted 1:1000, Santa Cruz Biotechnology), phospho-EGFR (diluted 1:1000, Cell Signaling Technologies), and

Table 1. FDA-Approved Drugs Utilized for This Study

Drugs	Targets
Dasatinib	Src, Bcr-Abl, c-kit
Paclitaxel	Microtubule
Lapatinib	EGFR
Sunitinib malate	VEGFR, PDGFR, C-kit, Flt
Ponatinib (AP24534)	Src, Abl, VEGFR2, FGFR1
OSI-420 (desmethyl erlotinib)	EGFR
Afatinib (BIBW2992)	EGFR, HER2
Erlotinib HCl	EGFR
Vincristine	Microtubules
Vinorelbine tartrate	Microtubules
Gefitinib (Iressa)	EGFR, Akt
Oxaliplatin (Eloxatin)	DNA/RNA synthesis
Zoledronic acid	RAS, Rho GTPases
Bosutinib (SKI-606)	Src, Akt
Sorafenib (Nexavar)	VEGFR, PDGFR, RAF/MEK/ERK
Masitinib (AB1010)	FAK, c-kit, PDGFR, FGFR
Docetaxel (Taxotere)	Microtubules
Fludaurabine phosphate (Fludara)	DNA/RNA synthesis
Ruxolitinib (INCB018424)	JAK
PCI-32765 (Ibrutinib)	Src

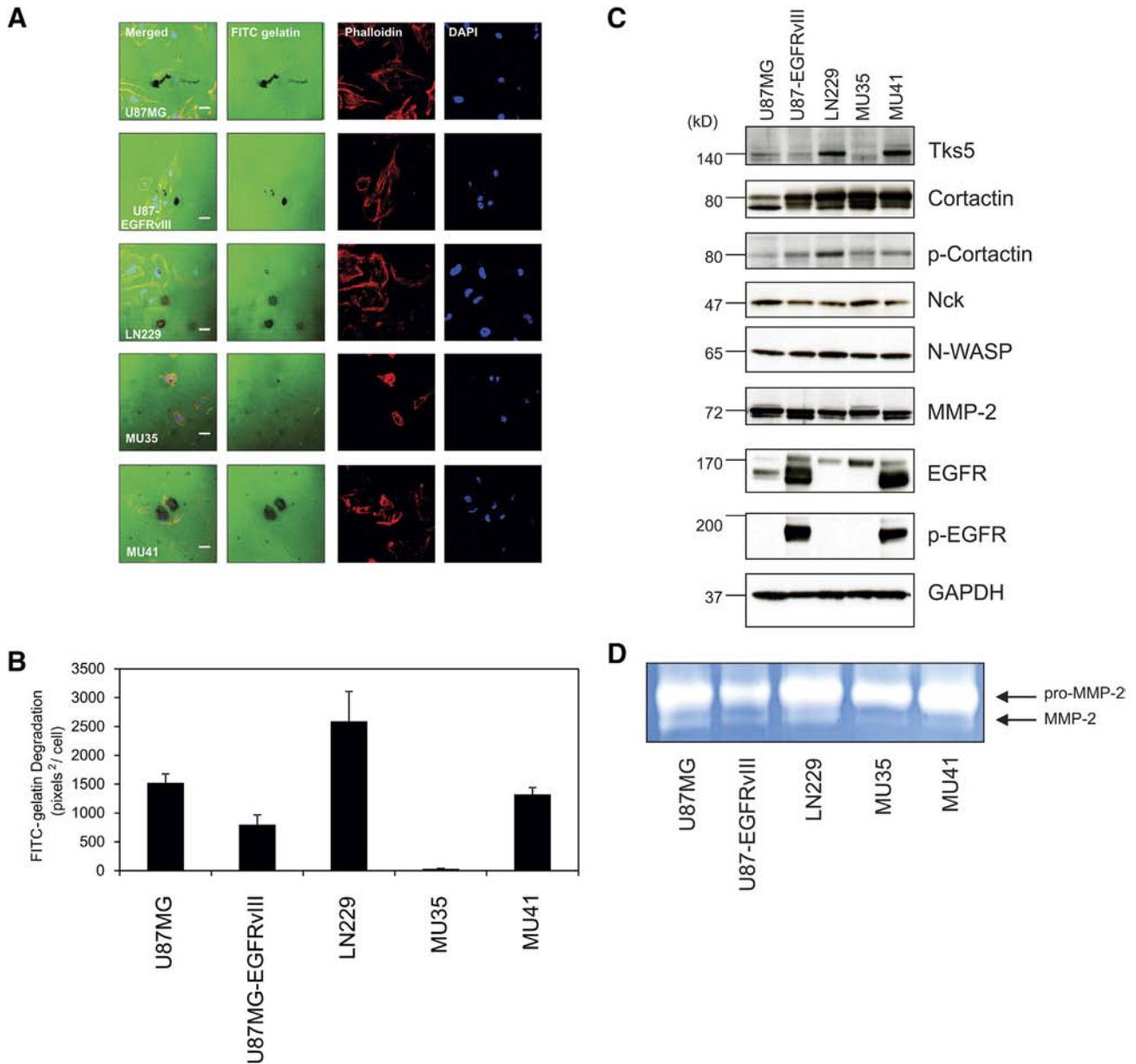


Figure 1. GBM cell lines express invadopodia regulators, form functional invadopodia and secrete MMP-2. (A) LN229, U87MG, U87MG-EGFRvIII, MU35 and MU41 GBM cells were plated on a thin film of cross-linked FITC-gelatin for 24 hours to detect the presence of invadopodia-mediated FITC-gelatin degradation. White scale bars represent 20 μ m. Mean FITC-labeled gelatin degrading activity of GBM cells. Degraded areas of FITC-labeled gelatin are evident as black areas devoid of FITC-labeled gelatin (green). DAPI staining of the nucleus is shown in blue, and rhodamine phalloidin (red) was used to stain for actin filaments and actin puncta (invadopodia). (B) Graph depicting the basal invadopodia-mediated FITC-gelatin degradation activity of the GBM cell lines in (A). Experiment repeated two times. (C) Immunoblot analysis of various regulators of invadopodia formation or activity in the listed GBM cell lines. The experiment was repeated twice, and representative images are shown. (D) Gelatin zymogram analysis showing MMP-2 activity at 24 hours after incubation of GBM cells in serum-free OptiMEM. The experiment was repeated twice, and a representative image is shown.

EGFR (diluted 1:1000, Cell Signaling Technologies). The membranes were then washed three times in 1 \times TBST for 5 minutes each wash and then incubated with the appropriate secondary antibody (1:10,000) (BioRad) and subsequently developed using enhanced chemiluminescence reagent (GE Healthcare) and exposure onto Super RX x-ray film (Fujifilm).

Gelatinase Zymography

For zymography analyses, 2 \times 10⁵ cells were seeded per well in six-well plates (Corning) and were allowed to adhere overnight before

washing with sterile PBS and subsequent incubation in serum-free OptiMEM (Thermofisher Scientific) for 24 hours. One-hundred-microliter aliquots of the conditioned OptiMEM medium was then sampled and centrifuged at 1000 \times g (4 $^{\circ}$ C) for 10 minutes before storage at -80 $^{\circ}$ C. Gelatin zymography was performed using 10% gelatin-substrate zymography NuPAGE precast gels (Invitrogen, Australia) and the conditioned OptiMEM media samples [which were normalized against the corresponding cell protein lysate concentrations, as determined using the BCA protein assay (Pierce, Thermofisher Scientific)]. The samples were then separated on the

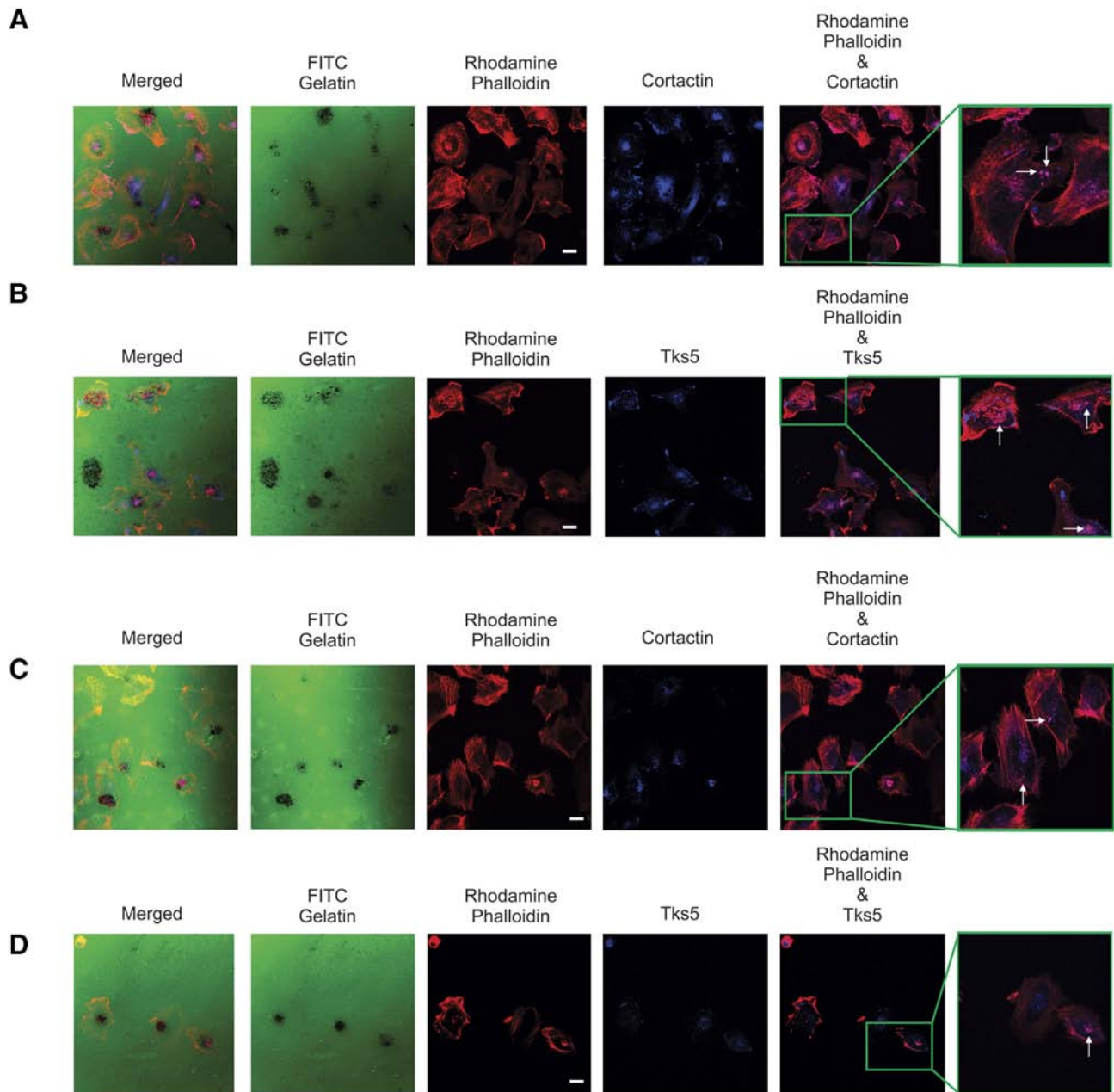


Figure 2. Endogenous cortactin and Tks5 colocalize to invadopodia actin puncta in LN229 and MU41 GBM cells. LN229 and MU41 GBM cells were plated on coverslips coated with a thin film of cross-linked FITC-labeled gelatin. After 24 hours, the cells were fixed and stained for actin filaments with rhodamine-phalloidin (red), cortactin, and Tks5 primary antibodies and an Alexa 405 secondary antibody (blue). Respective images are shown as follows: LN229 (A-cortactin) and (B-Tks5) and MU41 (C-cortactin) and (D-Tks5) GBM cells. The white arrows indicate co-localization of rhodamine phalloidin–stained actin puncta with cortactin or Tks5 within invadopodia. The experiment was repeated twice, and representative images are shown. Scale bar=20 μ m.

zymography precast gels by electrophoresis at 125 V for 1.5 hours in 1 \times Novex Tris-Glycine SDS Running Buffer. Gels were then removed and incubated for 30 minutes (RT) in 1 \times Novex zymogram renaturing buffer (ThermoFisher Scientific) followed by a further 30-minute incubation (RT) in 1 \times Novex zymogram developing buffer (ThermoFisher Scientific), which was then replaced with new developing buffer for overnight incubation at 37°C. Gels were subsequently washed in distilled water and stained for 1 hour in Simply-Blue Stain (Life Technologies) followed by further washing in distilled water until clear gelatinolytic bands were visible. The molecular weight was identified with the aid of loaded Precision Blue

protein markers (Bio-Rad). The gels were scanned using a flatbed scanner for further densitometric analysis using Image J (version 1.51f).

Cell Viability Assays

Cells were seeded into 96-well plates (1 \times 10⁴ cells/100 μ l) and were allowed to adhere overnight. Cells were treated with the FDA-approved drugs at increasing concentrations (0, 0.01, 0.1, 1, and 10 μ M in triplicate) for 72 hours in a humidified environment (10% CO₂ at 37°C). Cell viability after drug treatment was assessed on a plate reader (at a wavelength of 570 nm) using a CellTiter 96 Non-

Table 2. Invadopodia regulators Are Overexpressed in GBM Relative to Normal Brain Tissue

Invadopodia Marker	Cancer Tissue Sample	Number of Samples	Corresponding Tissue Sample	Number of Samples	Total Measured Genes	Mean Fold Change (Log2)	P Value	Sample Type	Platform	Study
Tks4	GBM	27	Normal brain	4	14,836	3.257	1.12E-04	mRNA	ND	Bredel Brain 2
MMP2	GBM	27	Normal brain	4	14,836	6.426	5.41E-04	mRNA	ND	Bredel Brain 2
Nck1	GBM	27	Normal brain	4	14,836	1.717	1.00E-02	mRNA	ND	Bredel Brain 2
Tks5	GBM	27	Normal brain	4	14,836	1.399	0.048	mRNA	ND	Bredel Brain 2
MMP2	GBM	30	Normal brain	3	9957	4.537	3.00E-03	mRNA	ND	Liang
Tks4	GBM	30	Normal brain	3	9957	1.492	1.40E-02	mRNA	ND	Liang
Nck1	GBM	30	Normal brain	3	9957	1.626	1.90E-02	mRNA	ND	Liang
Tks4	GBM	80	Normal brain	4	19,574	2.241	1.32E-06	mRNA	Human Genome U133 Plus 2.0 Array	Murat
MMP2	GBM	80	Normal brain	4	19,574	2.92	2.98E-04	mRNA	Human Genome U133 Plus 2.0 Array	Murat
Nck2	GBM	80	Normal brain	4	19,574	1.135	2.00E-03	mRNA	Human Genome U133 Plus 2.0 Array	Murat
Nck1	GBM	80	Normal brain	4	19,574	1.885	5.00E-03	mRNA	Human Genome U133 Plus 2.0 Array	Murat
Src	GBM	80	Normal brain	4	19,574	1.035	4.50E-02	mRNA	Human Genome U133 Plus 2.0 Array	Murat
MMP2	GBM	81	Normal brain	23	19,574	3.548	7.99E-16	mRNA	Human Genome U133 Plus 2.0 Array	Sun
Tks4	GBM	81	Normal brain	23	19,574	2.194	2.50E-04	mRNA	Human Genome U133 Plus 2.0 Array	Sun
Nck1	GBM	81	Normal brain	23	19,574	1.305	5.41E-07	mRNA	Human Genome U133 Plus 2.0 Array	Sun
Src	GBM	81	Normal brain	23	19,574	1.601	2.00E-03	mRNA	Human Genome U133 Plus 2.0 Array	Sun
NWASP	GBM	81	Normal brain	23	19,574	1.338	1.10E-02	mRNA	Human Genome U133 Plus 2.0 Array	Sun
MMP2	GBM	542	Normal brain	10	12,624	4.818	4.06E-10	mRNA	Human Genome U133A Array	TCGA
Nck1	GBM	542	Normal brain	10	12,624	2.056	4.00E-09	mRNA	Human Genome U133A Array	TCGA
Cortactin	GBM	542	Normal brain	10	12,624	1.353	0.003	mRNA	Human Genome Y133A Array	TCGA

mRNA expression levels of invadopodia regulators was examined in GBM and normal brain tissue within the Oncomine database. Displayed in this table are the mean fold changes versus normal brain in each study and overall P value in that dataset. Gene expression data are log transformed and normalized as previously described [41]. ND, not defined.

Radioactive Cell Proliferation Assay (MTT) (Promega) as per the manufacturer's instructions.

Invadopodia Degradation and Colocalization Assays

FITC-gelatin invadopodia/matrix degradation assays were performed as previously described [33]. For basal invadopodia activity screening of the GBM cell lines, 1 × 10⁵ cells were seeded per coverslip and incubated for 24 hours in a humidified environment (10% CO₂ at 37°C). The cells were then washed with 1× PBS and fixed in 4% paraformaldehyde for 15 minutes. The cells were next permeabilized with 0.2% Triton-X-100 and then stained with rhodamine phalloidin (invadopodia actin puncta) and DAPI (nucleus), and the coverslips were mounted with Vectashield (Vector Laboratories). Images were then acquired using a Nikon A1+ confocal microscope system utilizing a Plan Apo VC 60x Oil DIC N2 immersion objective. Degraded gelatin was defined as black areas depleted of fluorescent gelatin within each image. A total of 10-15 random image fields were acquired for each sample and saved in two image formats: native Nikon ND2 and an uncompressed jpeg format. Images were subsequently analyzed using ImageJ (version 1.51f, NIH), and threshold and region tools were utilized to define the total region of degradation present within each acquired image field. A particle counter macro was then employed to calculate the total area of FITC-conjugated gelatin degradation, and this was then standardized relative to the number of DAPI-positive cells that were present within the image field. Experiments investigating the effect of FDA-approved agents on invadopodia activity were as follows: LN229 cells were irradiated at 2 Gy and treated with 200 μM of TMZ for 24 hours (10% CO₂/37°C). The cells were then treated with 0.01 μM of an FDA-approved drug for an additional 72 hours (10% CO₂/37°C). The cells were then trypsinized and seeded at a density of 1 × 10⁵ cells per FITC-gelatin coated coverslip for 24 hours in the absence of drug (10% CO₂/37°C) prior to fixing and staining as previously outlined.

In Vitro Scratch Wound Assay

Cells were seeded into 6-well plates (3 × 10⁵ cells/well) and left to adhere overnight in a humidified environment (10% CO₂ at 37°C).

They were then treated for 72 hours with 0.01 μM of drug, after which 5 μg/ml of Mitomycin C (2 hours, 10% CO₂/37°C) was then added to the cells to arrest proliferation, followed by the introduction of a scratch 2 hours later. The cells were then washed twice in PBS before fresh medium was added. Images were acquired at time points 0, 6, and 24 hours using a 4× objective. Images were analyzed using ImageJ (Version 1.51f) in order to define the area of the wound.

Results

GBM Cell Lines Are Able to Form Functional Invadopodia

Invadopodia are actin-rich membrane protrusions that served as mediators of cell invasion due to their ability for concentrating and secreting metalloproteinases [8,33]. Therefore, initial investigations involved whether the GBM cell line panel possessed the ability to form functional matrix-degrading invadopodia through the use of the FITC-gelatin degradation assays. Figure 1A shows that the five GBM cell lines are able to form functional FITC-gelatin degrading invadopodia, as indicated by the presence of darkened areas devoid of FITC-labeled gelatin, colocalized with rhodamine phalloidin-stained actin puncta. Furthermore, quantification of the level of degradation varied, with the LN229 cell line exhibiting the greatest amount of FITC-gelatin degradation and the in-house patient-derived GBM cell line MU35 the least (Figure 1B).

Importantly, there are a range of different proteins that facilitate the initiation, formation, and regulation of the activity of invadopodia [10,34]. This led us to investigate the expression levels of a number of these regulatory invadopodia-related proteins in our GBM cell lines, including Tks5, cortactin, phospho-cortactin, Nck, N-WASP, MMP-2, EGFR, and phospho-EGFR (Figure 1C). The protein expression profiles of the regulators varied across the cell lines; however, relatively uniform levels of MMP-2, Nck, and N-WASP were observed across the cell lines. The cell line which displayed the most invadopodia-mediated FITC-gelatin degradation, LN229, expressed high levels of the invadopodia proteins phospho-cortactin, cortactin, and Tks5. It has been shown that Tks5 can function as a tether which mediates Rab40b-dependent MMP-2 transport vesicle

Table 3. Shortlisted FDA-Approved Drugs Exhibiting Greatest Reduction in GBM Cell Viability

Target	Drug	Greatest Cell Viability Reduction Efficacy
10 μM FDA-approved drug group		
Src	Ponatinib	5 / 5 cell lines
VEGFR, PDGFR	Sorafenib	5 / 5 cell lines
Src	Bosutinib	5 / 5 cell lines
DNA/RNA synthesis	Fludarabine phosphate	5 / 5 cell lines
EGFR	Afatinib	2 / 5 cell lines
EGFR	Lapatinib	1 / 5 cell lines
VEGFR, PDGFR	Sunitinib Malate	1 / 5 cell lines
1 μM FDA-approved drug group		
DNA/RNA synthesis	Fludarabine phosphate	5 / 5 cell lines
Microtubules	Paclitaxel	5 / 5 cell lines
Src	Ponatinib	3 / 5 cell lines
Microtubules	Vinorelbine tartrate	3 / 5 cell lines
Src	Dasatinib	2 / 5 cell lines
Src	Bosutinib	2 / 5 cell lines
Microtubules	Docetaxel	1 / 5 cell lines
VEGFR, PDGFR	Sunitinib malate	1 / 5 cell lines
Microtubules	Vincristine	1 / 5 cell lines
VEGFR, PDGFR	Sorafenib	1 / 5 cell lines
0.1 μM FDA-approved drug group		
Microtubules	Paclitaxel	5 / 5 cell lines
Microtubules	Vinorelbine tartrate	5 / 5 cell lines
DNA/RNA synthesis	Fludarabine phosphate	4 / 5 cell lines
Src	Dasatinib	3 / 5 cell lines
Microtubules	Docetaxel	2 / 5 cell lines
Src	PCI-32765	1 / 5 cell lines
RAS, Rho GTPases	Zoledronic acid	1 / 5 cell lines
Src	Ponatinib	1 / 5 cell lines
EGFR	Afatinib	1 / 5 cell lines
Src	Bosutinib	1 / 5 cell lines
VEGFR, PDGFR	Sorafenib	1 / 5 cell lines
0.01 μM FDA-approved drug group		
Microtubules	Vinorelbine tartrate	5 / 5 cell lines
Microtubules	Docetaxel	4 / 5 cell lines
Src	Dasatinib	4 / 5 cell lines
Microtubules	Paclitaxel	4 / 5 cell lines
Microtubules	Vincristine	3 / 5 cell lines
DNA/RNA synthesis	Fludarabine phosphate	2 / 5 cell lines
EGFR	Afatinib	1 / 5 cell lines
VEGFR, PDGFR	Sorafenib	1 / 5 cell lines
JAK	Ruxolitinib	1 / 5 cell lines

targeting to the invadopodia tip [35]. This is in addition to the correlation of cortactin levels in head and neck squamous carcinoma cell lines and the degree of secretion/activation of MMPs at the invadopodia tip, influencing the degree of ECM degradation [36]. This is in contrast to cell line MU35, which displayed lower levels of Tks5 and phospho-cortactin, as well decreased levels of FITC-gelatin degradation. Free actin barbed generation combined with actin polymerization that is involved in the stabilization and maturation of invadopodia formation can also be facilitated by EGFR-mediated signaling [37], and a range of total and phospho-EGFR protein levels can be observed in the GBM cell line panel.

Invadopodia-mediated invasion is aided by the recruitment of proteases [matrix metalloproteinases (MMPs)] to the tip of the invadopodium where they are subsequently secreted and activated in order to proteolytically degrade the surrounding ECM. Using zymography, we are able to assess the extracellular enzymatic activity of these secreted proteases, as seen in Figure 1D. Analysis conducted on the conditioned media from GBM cell lines at 24 hours revealed that the prominent MMP forms identified were pro-MMP-2 (72 kDa) and active MMP-2 (65 kDa). In addition to the increased levels

of phospho-cortactin, cortactin, and Tks5 observed in the LN229 cell line, it can also be seen that the active form of MMP-2 was also elevated, indicating that this combination may have contributed to the increased FITC-gelatin degradation activity. In contrast, the MU35 cell line displayed decreased levels of active MMP-2 coupled with lower protein expression levels of Tks5 and phospho-cortactin, potentially contributing to the observed lower levels of FITC-gelatin degradation (Figure 1A/B).

Through the utilization of confocal microscopy, invadopodia can be identified by the colocalization of regulatory proteins such as cortactin or Tks5 with actin puncta and areas of degraded FITC-gelatin [33,38]. Therefore, we confirmed the presence of active invadopodia through the colocalization of the invadopodia-regulating proteins cortactin and Tks5 with actin puncta with degraded areas of FITC-gelatin, as seen in the representative images of the LN229 cells (Figure 2).

GBM Tissue Can Exhibit Increased mRNA Expression of Multiple Invadopodia Regulators

We examined the potential clinical significance of invadopodia in GBM by utilizing the online Oncomine platform for datasets that contained mRNA expression levels in GBM and normal brain for a number of genes that are involved in the regulation of invadopodia. These included Tks5, Tks4, cortactin, Nck1, NWASP, Src, and MMP-2. Oncomine (version 4.5, www.oncomine.org, Compendia Bioscience, Ann Arbor, MI, USA, Thermo Fisher) is an online tool that contains 715 mRNA and copy number expression datasets from 86,733 cancer and normal tissue samples [39]. Datasets were examined from five independent GBM studies which showed a significant increase in the mRNA expression levels of a number of invadopodia regulators in GBM tissue samples compared to normal brain samples (Table 2). It was observed that MMP-2 and Nck1 were the most frequently overexpressed regulators across all five studies, followed by Tks4 and Src. We also carried out co-expression analyses (Supplementary Figure 1) which revealed that more than one invadopodia regulator may be overexpressed in a single GBM sample relative to low mRNA expression levels in normal brain. The increased mRNA expression of various invadopodia regulators in GBM tissue highlights the potential clinical significance of these structures in GBM patients. It also supports our previous evidence associating invadopodia with glioma cells [11,15].

FDA-Approved Drugs Reduce GBM Cell Line Viability

Although the current therapeutic approach of radiotherapy and concomitant temozolomide postsurgery for GBM provides a modest improvement in survival, only 26.5% of individuals remain alive at 2 years due to tumor recurrence and invasion [40]. Therefore, there is an urgent need to develop new therapies to complement the current clinical protocol in targeting cells that may survive radiotherapy and TMZ. As the activity of invadopodia is known to facilitate the invasive ability of tumor cells [10,30], we examined a panel of 20 FDA-approved agents with known targets that would potentially have an impact on invadopodia-related regulatory pathways (Table 1). In addition to screening for a drug that may possess an “anti-invadopodia” property, we initially short-listed the drugs based on their potential to reduce glioma cell viability posttreatment. This would allow us to possibly uncover an FDA-approved drug, not previously used in the treatment of GBM patients, that had a dual effect (cytotoxic and anti-invadopodia) on GBM cells that survived

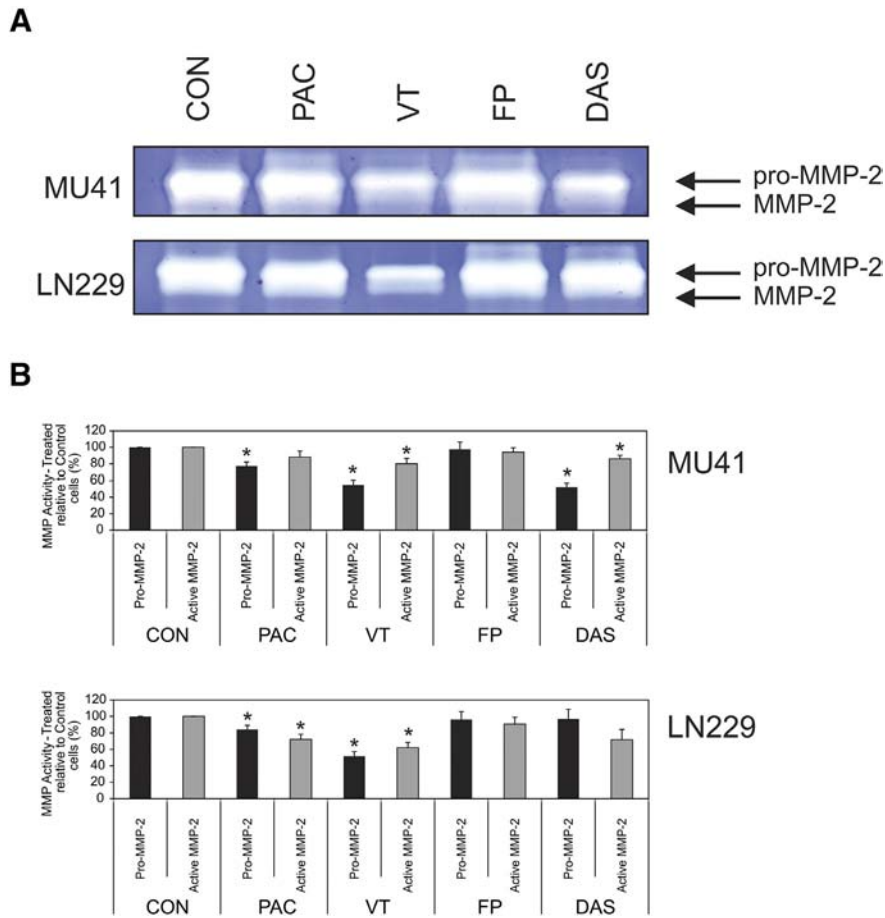


Figure 3. Vinorelbine tartrate and paclitaxel can reduce MMP-2 secretion in GBM cells.(A) Gelatin-based zymogram analysis of serum-free OptiMem conditioned medium showing MMP-2 secretion activity of MU41 and LN229 GBM cells treated with 0.01 μ M paclitaxel (PAC), vinorelbine tartrate (VT), fludarabine phosphate (FP), or dasatinib (DAS) [untreated control (CON)] for 24 hours. The experiment was repeated twice, and a representative image is shown. (B) Densitometric analysis of zymograms.

RT and TMZ. The chemotherapeutic sensitivity of the five GBM cell lines was assessed with the 20 FDA-approved drugs across a range of concentrations (0, 0.01, 0.1, 1, and 10 μ M). A variable response to the FDA-approved drugs over the concentration range was observed with the five GBM cell lines (Supplementary Figure 3). We then ranked the responses based on the level of reduction in cell viability across as many cell lines as possible for each drug concentration (Table 3). For further analysis, the four most effective drugs at the concentration of 0.1 μ M (paclitaxel, vinorelbine tartrate, dasatinib, and fludarabine phosphate) were selected, which were also effective at reducing cell viability at the other concentrations.

Vinorelbine Tartrate and Paclitaxel Can Reduce MMP-2 Secretion, Invadopodia-Mediated Degradation, and Migration in GBM Cells

As we had observed earlier that the GBM cell lines were able to secrete MMP-2 and form functional FITC-gelatin degrading invadopodia, we investigated the impact of the four drugs (paclitaxel, vinorelbine tartrate, dasatinib, and fludarabine phosphate) on these processes at a lower concentration of 0.01 μ M on two cell lines, LN229 and MU41. Vinorelbine- or paclitaxel-treated LN229 and MU41 cells showed a decrease in MMP-2 secretion relative to the untreated control cells (Figure 3). Interestingly, dasatinib treatment

resulted in a reduced secretion of MMP-2 in the MU41 cells and not the LN229 cells. Subsequently, we examined the effect of these agents on the invadopodia-mediated FITC-gelatin degradation ability of the GBM cells. It was observed that vinorelbine tartrate was effective at significantly reducing the invadopodia-mediated degradation activity of both cell lines (Figure 4). This was consistent with the reduction in MMP-2 secretion and was also observed with paclitaxel-treated cells (however, the reduction in degradation was only significant in the LN229 cell line).

As a number of the invadopodia regulators such as cortactin are known to also be involved in modulating cell movement, due to their dynamic interactions with the actin cytoskeleton, we also examined the effect of the short-listed drugs on cellular migration. This was only investigated with the LN229 cell line (not the MU41 cell line) due to its ability to form a compact confluent monolayer suitable for the scratch wound assay. As can be seen in Figure 5, both vinorelbine tartrate and paclitaxel were effective in significantly reducing the migratory capacity of the LN229 cell line relative to the untreated control. We also examined the effect of three additional drugs on LN229 cell migration including ponatinib, sorafenib, and bosutinib (as they exhibited efficient reductions in cell viability across the five GBM cell lines at the highest drug concentration of 10 μ M but were less effective at the lower concentrations). These three drugs were not

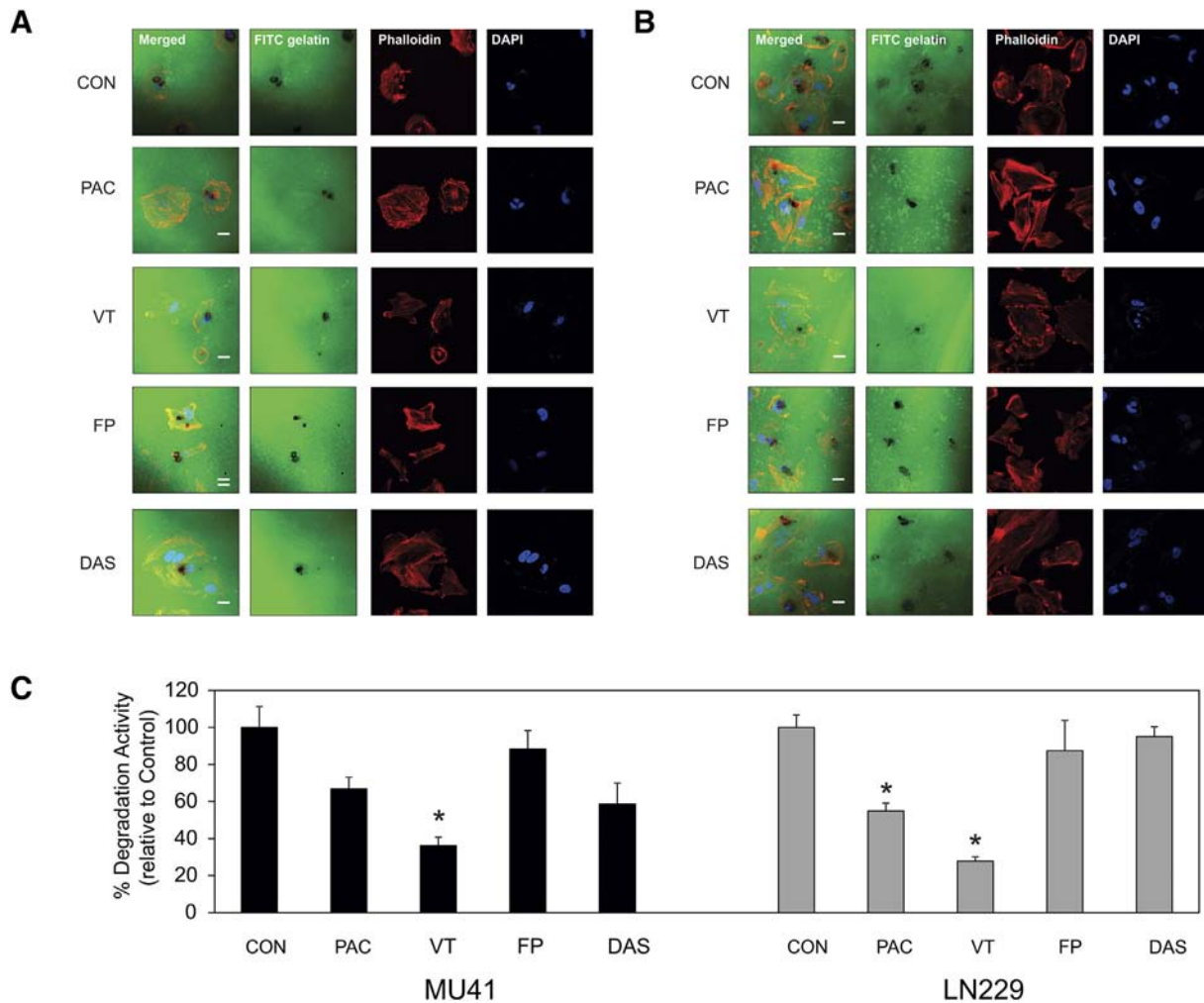


Figure 4. Vinorelbine tartrate and paclitaxel can reduce invadopodia activity in GBM cells. (A) MU41 and (B) LN229 GBM cells were plated on coverslips coated with a thin film of cross-linked FITC-labeled gelatin 24 hours posttreatment with 0.01 μ M dasatinib (DAS), fludarabine phosphate (FP), paclitaxel (PAC), or vinorelbine tartrate (VT) [untreated control (CON)]. After an additional 24 hours, the cells were subsequently fixed and stained for actin filaments with rhodamine-phalloidin (red) and DAPI nuclear staining (blue). Degraded areas of FITC-labeled gelatin are evident as black areas devoid of FITC-labeled gelatin (green). The mean FITC-labeled gelatin degrading activity (relative to the untreated control) was determined (C). * $P < .05$ versus control. The experiment was repeated two times, and representative images are shown. Scale bar = 20 μ m.

effective at reducing the migratory capacity of the LN229 cell line over 24 hours, as were dasatinib, paclitaxel, and vinorelbine tartrate.

MMP-2 Secretion and Invadopodia-Mediated FITC-Gelatin Degradation Is Enhanced by Radiation and TMZ

It is known that there are a number of stages involved in the formation and activity of invadopodia [34] including the following: Stage I, early precursor or initiation stage; Stage II, late precursor or preinvadopodia; Stage III, early mature invadopodia; and Stage IV, late mature invadopodia. These stages comprise the various processes of invadopodium core structure formation, maintenance of actin polymerization for structure stability, and recruitment of regulatory and functional proteins including the MMPs, which are subsequently secreted from the invadopodial tip to promote degradation of the surrounding ECM. As the LN229 cell line readily forms FITC-gelatin degrading invadopodia and shows the highest level of activity from our cell line panel, it was treated with 2 Gy RT and 200 μ M of

TMZ, and the effect on MMP-2 secretion via zymographic analysis was examined. As can be seen in Supplementary Figure 2A, there is an increase in MMP-2 secretion posttreatment with RT and TMZ. A number of studies have reported that GBM cells surviving RT and TMZ treatment can display enhanced migratory and invasive potential [24,25,28], indicating that the long-term inadequacy of treatment observed for most patients may be related to surviving cells exhibiting an increased invasive capacity. As there was an increase in MMP-2 secretion post-RT/TMZ treatment, we next investigated whether RT/TMZ treatment would result in a functional change in the level of invadopodia activity. FITC-conjugated gelatin degradation assays utilizing RT/TMZ-treated LN229 cells revealed a significant increase in the invadopodia-mediated degrading ability of the cells post-RT/TMZ treatment compared to the untreated control (Supplementary Figure 2B). This is in accordance with the observed increase in MMP-2 secretion and highlights that GBM cells which survive treatment may potentially possess a proinvasive

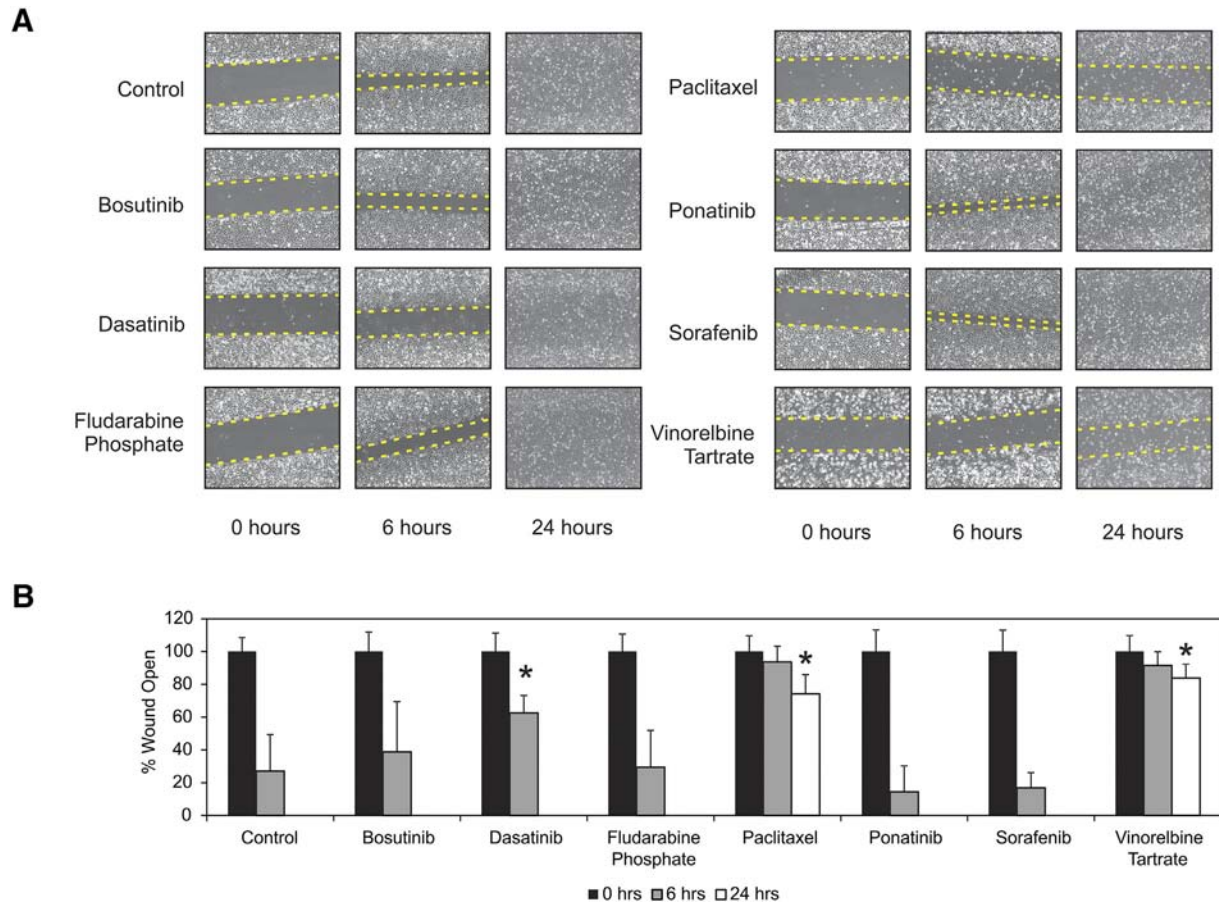


Figure 5. Vinorelbine tartrate and paclitaxel can reduce GBM cell migration. LN229 GBM cells were treated with 0.01 μM bosutinib, dasatinib, fludarabine phosphate, paclitaxel, ponatinib, sorafenib, or vinorelbine tartrate for 72 hours followed by 5 $\mu\text{g}/\text{ml}$ mitomycin c for 2 hours. A scratch wound was introduced into the confluent monolayer, and images were acquired at 0, 6, and 24 hours. The wound area for each time point was determined relative to $t=0$ hour. * $P<.05$ versus control. The experiment was repeated two times, and representative images are shown.

phenotype and that this may be mediated through the activity of invadopodia.

Vinorelbine Tartrate and Paclitaxel Can Reduce Radiotherapy- and Temozolomide-Induced Invadopodia-Mediated Activity in GBM Cells

The presence of invadopodia on tumor cells has been identified in both *in vitro* and *in vivo* environments, contributing to the matrix degradation process which ultimately can facilitate cellular invasion [10,34,36]. As we had identified that paclitaxel and vinorelbine tartrate were both able to reduce invadopodia-mediated FITC-gelatin degradation in GBM cells, we wanted to determine if their “anti-invadopodia” effect could be reproduced in cells that had been pretreated with RT/TMZ (which show augmented invadopodia activity in the surviving cells). This is a critical point, as it identifies the possibility that an “anti-invadopodia” or “anti-invasive” drug that is already FDA-approved could conceivably be adapted to the existing clinical treatment of GBM patients. As the LN229 cell line exhibited the greatest level of invadopodia-mediated FITC-gelatin degradation (Figure 1D), we examined the effect of paclitaxel and vinorelbine tartrate on RT/TMZ-treated LN229 cells. In addition to these two agents, we also investigated the “anti-invadopodia” effect on RT/TMZ-treated LN229 cells of a number of the other drugs which were effective at reducing cell viability across multiple cell lines at

concentrations of 0.1 or 10 μM , including bosutinib, sorafenib, and ponatinib (10 μM group) and dasatinib and fludarabine phosphate (0.1 μM) (Table 3). As can be observed in Figure 6, there was a significant increase in invadopodia-mediated FITC-gelatin degradation activity in RT/TMZ-treated LN229 cells relative to the untreated control. Treatment with vinorelbine tartrate or paclitaxel resulted in a reduction of RT/TMZ-induced invadopodia activity in the LN229 cells. This was also observed with the drug bosutinib; however, the greatest reduction in FITC-gelatin degradation was observed with vinorelbine tartrate.

Discussion

Despite advances in the treatment of GBM, the median survival time is 14.6 months for GBM patients, with tumor recurrence contributing to the poor patient outcome [41]. The highly infiltrative nature of GBM cells, limits complete surgical resection and exposure to chemotherapeutics due to reduced tissue penetrance. There is also limited exposure to radiation treatment of these invasive cells in normal brain, due to the narrow therapeutic index of radiation therapy to prevent radiation-induced toxicity in the surrounding normal brain. Ultimately, this allows for the formation of tumor satellites at distant locations from the primary tumor following therapy, resulting in treatment failure and facilitating tumor relapse.

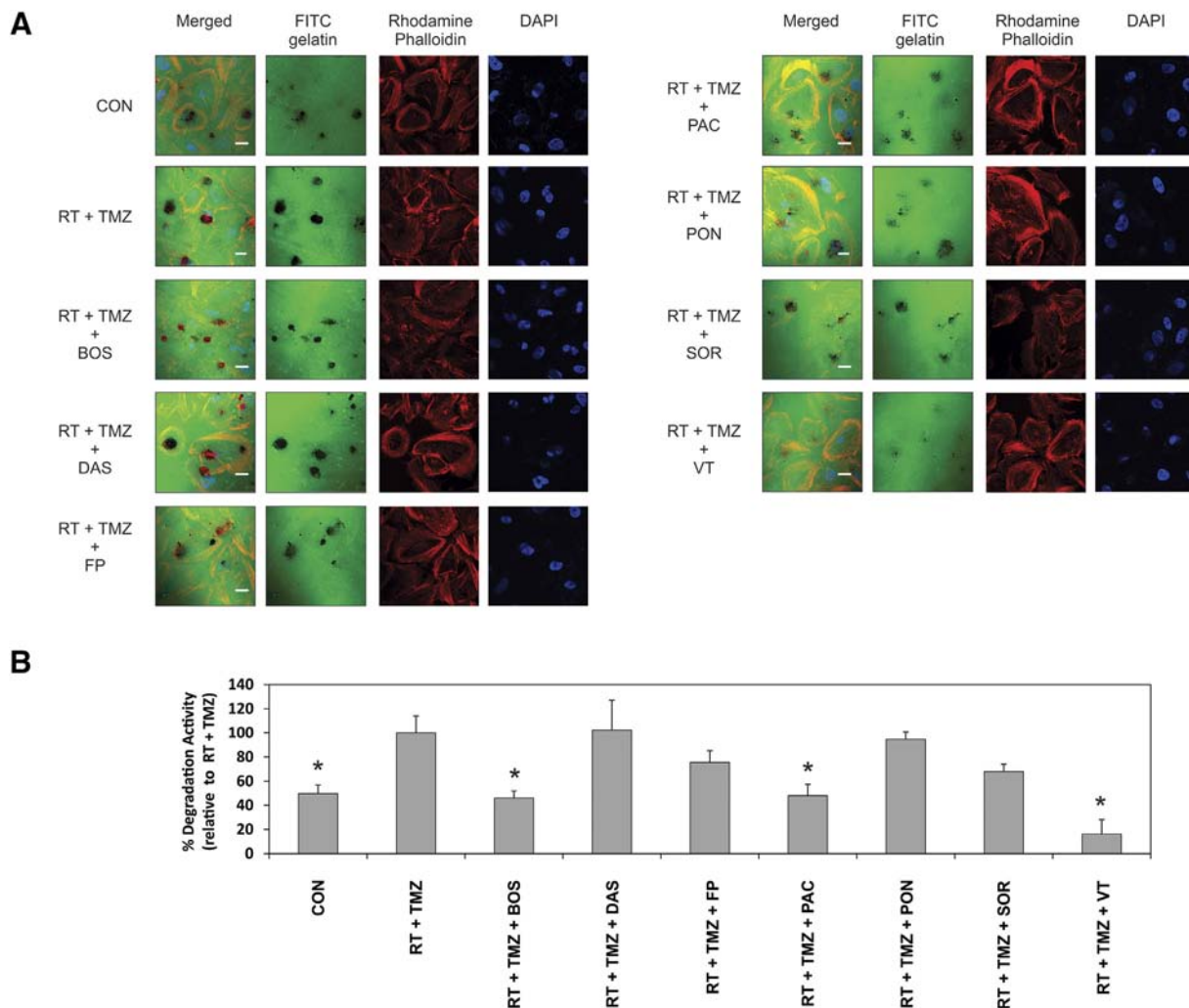


Figure 6. Vinorelbine tartrate and paclitaxel can reduce radiotherapy- and temozolomide-induced invadopodia-mediated activity in LN229 GBM cells. LN229 GBM cells were treated with RT/TMZ (2 Gy/200 μ M) 24 hours prior to the addition of 0.01 μ M bosutinib (BOS), dasatinib (DAS), fludarabine phosphate (FP), paclitaxel (PAC), ponatinib (PON), sorafenib (SOR), or vinorelbine tartrate (VT) and prior to being plated on coverslips coated with a thin film of cross-linked FITC-gelatin. After an additional 24 hours, the cells were subsequently fixed and stained for actin filaments with rhodamine-phalloidin (red) and DAPI nuclear staining (blue). Degraded areas of FITC-labeled gelatin are evident as black areas devoid of FITC-labeled gelatin (green). The mean FITC-labeled gelatin degrading activity (relative to the RT + TMZ treated cells) was determined (C). * $P < .05$ versus control. The experiment was repeated three times, and representative images are shown. Scale bar = 20 μ m.

Augmented migratory and invasive abilities of cancer cells result in establishing satellite or secondary tumors distant from the primary tumor mass. Importantly, membrane structures known as invadopodia have been documented to assist in cancer cell invasion and have also been observed in a number of cancers [36,37,42–50], including glioma [15]. These membrane protrusions have emerged as important facilitators of cancer cell invasion, serving to proteolytically degrade the surrounding ECM, thereby creating paths in which invading tumor cells migrate away from the primary tumor mass. The invasive capacity of cancer cells has been linked to their ability to form functional, matrix-degrading invadopodia; therefore, regulators of invadopodia formation and activity have been proposed to possess diagnostic or prognostic potential [15,42]. In the present study, data extracted from the Oncomine database revealed mRNA overexpression of multiple invadopodia regulators in GBM tissue (Table 1), highlighting the significance of these structures.

Clinical treatments may aid or accelerate the invasive capabilities of tumor cells, and recent studies have revealed a link between the current therapeutic approach, consisting of radiation and temozolomide, and enhanced migratory and invasive potential in GBM cells [22,23,26]. A study by Steinle et al. [51] demonstrated an increase in the extracellular secretion of MMP-2 in glioma cell lines that were exposed to radiation, which correlated with an enhanced invasive capacity (and increased levels of MMP-2 protein expression) into surrounding normal brain tissue when the irradiated cells were subsequently implanted into rat brains. MMP-2 is a member of the matrix metalloproteinase family belonging to a class of zinc-dependent proteases that can degrade different proteins, including gelatin and collagen. Importantly, MMP-2 and MMP-9 are overexpressed in gliomas [52] and can be regulated by signaling via the EGFR and Src, both of which are important in the phosphorylation of several invadopodia regulators, thus leading to the localized matrix degradation of the ECM mediated by the secretion of these MMPs from the invadopodial tip [10].

Furthermore, studies investigating the effect of both radiotherapy (2 Gy) and TMZ (30 μ M) on U87MG GBM cells showed that treated cells exhibited enhanced MMP-2 activity [26,27]. Similar findings were reported in our previous study in which GBM cells that survived sublethal doses of radiation (2 Gy) and TMZ (1000 μ M) exhibited enhanced MMP-2 secretion and increased invadopodia formation and activity [28]. The data presented here showing that exposure of GBM cells to 2 Gy and a lower TMZ concentration (200 μ M) support the previous findings, highlighting the urgent need for exploring novel therapeutic strategies to target invadopodia formation in resistant GBM cells after RT/TMZ treatment.

Since there was increased invadopodia activity in GBM cells post-RT/TMZ, our aim was to target this RT/TMZ-induced invadopodia-mediated matrix degradation by investigating a panel of 20 FDA-approved agents with known targets that may impact on invadopodia-related pathways (Table 2). Importantly, the focus of our study was to identify drugs that can act “dualistically” as both cytotoxic and “anti-invadopodia” agents against GBM cells that survive radiotherapy and TMZ treatment that exhibit enhanced invadopodia activity, which would facilitate the establishment of tumor satellites distant from the primary tumor resection site.

Our study identified two FDA-approved drugs, paclitaxel (currently approved for a variety of solid cancers, particularly breast and ovarian [53]) and vinorelbine tartrate (approved for non-small cell lung cancer [54,55]), as possessing a number of characteristics that allow them to be categorized as “dualistic” agents. Firstly, they were effective at causing a reduction in cell viability in all GBM cell lines at a lower drug concentration of 0.1 μ M but were also effective at 0.01 μ M. This is a crucial key as administered drugs can be metabolized/excreted and the blood-brain barrier can hinder the penetration of a drug to the tumor, leading to low drug levels being present within the tumor [56]. Secondly, these two agents had an impact on reducing the secreted levels of MMP-2, which facilitate invadopodia-mediated ECM degradation [10,11,34]. A decrease in the migration rate of the LN229 GBM cells was also observed, but importantly, in terms of a “dualistic” effect, these two agents were also able to reduce the RT/TMZ-induced invadopodia-mediated FITC-gelatin degradation. Notably, both vinorelbine tartrate and paclitaxel primarily target microtubules [48,57].

Microtubules play an important role in cell division and the maintenance of cellular structure, as well as serving to form a network along which secretory vesicles may be trafficked to the cell surface, such as those containing MMPs to be transported to the tip of the invadopodium for secretion and subsequent degradation of the surrounding ECM. Furthermore, microtubules also assist in stabilizing the invadopodium core, which is used to generate a protrusive force during elongation of invadopodia [10]. Vinorelbine tartrate and paclitaxel target microtubules in opposing approaches; vinorelbine prevents their assembly by binding to tubules and inhibiting their polymerization [58], while paclitaxel hyperstabilizes microtubules and hence prevents their disassembly [59]. In the case of paclitaxel, hyper-stabilization impedes the ability of microtubules to shorten and lengthen, which is necessary for their role as a molecule transport highway to the cell membrane [60], whereas vinorelbine hinders microtubule assembly and prevents a phenomenon known as “treadmilling” that involves active dynamics and microtubule lengthening through the addition of tubulin subunits at one end of the microtubule [61]. Interestingly, vinorelbine tartrate selectively binds to, and disrupts, mitotic microtubule proteins over axonal microtubules, making it less neurotoxic than other vinca alkaloids. It is possible that by targeting microtubules, these two drugs impede the

degrading capabilities of invadopodia by hindering the formation of a mature invadopodia core structure and also, potentially, the delivery of proteolytic enzymes such as MMP-2 to the tip of the invadopodium where it may be secreted into the extracellular space, facilitating degradation of the surrounding ECM.

Several studies have investigated the concomitant delivery of paclitaxel with radiation in patients with GBM. Ashamalla et al. [62] observed that the concomitant administration of paclitaxel with radiotherapy to GBM patients was well tolerated and resulted in an overall survival of 14 months. Julka et al. [63] also reported on a similar treatment approach in GBM patients and showed that the overall survival rate at 1 year was 70% with a combined paclitaxel/radiotherapy treatment approach. The median survival was reported to be at least 13 months at the closure of the study. While the survival rates for the combination of paclitaxel/radiotherapy are similar to what was achieved in the reported study by Stupp (radiotherapy/temozolomide) [40], it must be noted that the Stupp protocol also includes 6 months of temozolomide treatment postradiotherapy/concomitant temozolomide. Furthermore, a Brown University Oncology Group study used a paclitaxel-poly-L-glutamic acid conjugate to treat GBM patients in conjunction with radiotherapy and temozolomide [64]. The progression-free survival was 11.5 months, but importantly, the median overall survival was observed to be 18 months.

Vinorelbine tartrate has not been investigated clinically; however, a single case study of a female GBM patient receiving intravenous vinorelbine resulted in a progression-free interval extending beyond 24 months [65]. Encouragingly, it has been shown that vinorelbine tartrate is able to cross the blood-brain barrier in a preclinical model of brain metastases of breast cancer [57]. Pharmacokinetic analysis of plasma, blood, and tissue showed that, within 0.5 hour, the average concentration of vinorelbine in the brain metastases was 1.8 μ M (ranging up to 6.5 μ M), and at 8 hours, the concentration was still at 0.52 μ M (maximum at 5.8 μ M). This is extremely promising as the blood-brain barrier is compromised in GBM patients, and the concentrations of vinorelbine detected in the brain metastases from the Samala study fall within the efficacious cell viability and “anti-invadopodia” concentrations of vinorelbine in our current study.

In conclusion, the data from our current study investigating the role of repurposing FDA-approved agents indicate that a promising role exists for the two shortlisted agents, paclitaxel and vinorelbine tartrate, as novel prospective therapeutic agents that have the potential to be utilized as dual “chemotherapeutic” and “anti-invasive” (invadopodia) agents in targeting invasive GBM cells that survive RT and TMZ.

Supplementary data to this article can be found online at <https://doi.org/10.1016/j.tranon.2018.08.012>.

Acknowledgements

This work was supported by the following funding sources: Perpetual IMPACT Philanthropy Grant IPAP2017/0766 and The Royal Melbourne Hospital Neuroscience Foundation.

References

- [1] Ostrom QT, Gittleman H, Fulop J, Liu M, Blanda R, Kromer C, Wolinsky Y, Kruchko C, and Barnholtz-Sloan JS (2015). CBTRUS statistical report: primary brain and central nervous system tumors diagnosed in the United States in 2008-2012. *Neuro-Oncology* 17(Suppl. 4), iv1-iv62.
- [2] Omuro A and DeAngelis LM (2013). Glioblastoma and other malignant gliomas: a clinical review. *JAMA* 310(17), 1842-1850.
- [3] Siegel RL, Miller KD, and Jemal A (2018). Cancer statistics, 2018. *68*(1), 7-30.

- [4] A.I.o.H.a.W (2017). Brain and other central nervous system cancers. Cat no CAN 106. AIHW; 2017.
- [5] Hess CF, Schaaf JC, Kortmann RD, Schabert M, and Bamberg M (1994). Malignant glioma: patterns of failure following individually tailored limited volume irradiation. *Radiother Oncol* **30**(2), 146–149.
- [6] Stupp R, Brada M, van den Bent MJ, Tonn JC, and Pentheroudakis G (2014). High-grade glioma: ESMO clinical practice guidelines for diagnosis, treatment and follow-up. *Ann Oncol* **25**(Suppl. 3), iii93–iii101.
- [7] Thakkar JP, Dolecek TA, Horbinski C, Ostrom QT, Lightner DD, Barnholtz-Sloan JS, and Villano JL (2014). Epidemiologic and molecular prognostic review of glioblastoma. *Cancer Epidemiol Biomark Prev* **23**(10), 1985–1996.
- [8] Stupp R, Mason WP, van den Bent MJ, Weller M, Fisher B, Taphoorn MJB, Belanger K, Brandes AA, Marosi C, and Bogdahn U, et al (2005). Radiotherapy plus concomitant and adjuvant temozolomide for glioblastoma. *N Engl J Med* **352**(10), 987–996.
- [9] Khosla D (2016). Concurrent therapy to enhance radiotherapeutic outcomes in glioblastoma. *Ann Transl Med* **4**(3), 1–8 54.
- [10] Murphy D and Courtneidge S (2011). The 'ins' and 'outs' of podosomes and invadopodia: characteristics, formation and function. *Nat Rev Mol Cell Biol* **12** (7), 413–426.
- [11] Stylli S, Kaye A, and Lock P (2008). Invadopodia: At the cutting edge of tumour invasion. *J Clin Neurosci* **15**(7), 725–737.
- [12] Kelly T, Yan Y, Osborne R, Athota A, Rozypal T, Colclasure JC, and Chu W (1998). Proteolysis of extracellular matrix by invadopodia facilitates human breast cancer cell invasion and is mediated by matrix metalloproteinases. *Clin Exp Metastasis* **16**(6), 501–512.
- [13] Chuang Y-Y, Tran N, Rusk N, Nakada M, Berens M, and Symons M (2004). Role of synaptotagmin 2 in glioma cell migration and invasion. *Cancer Res* **64**(22), 8271–8275.
- [14] Cheerathodi M, Avci N, Guerrero P, Tang L, Popp J, Morales J, Chen Z, Carnero A, Lang F, and Ballif B, et al (2016). The cytoskeletal adapter protein spinophilin regulates invadopodia dynamics and tumor cell invasion in glioblastoma. *Mol Cancer Res* **14**(12), 1277–1287.
- [15] Styll SS, I ST, Kaye AH, and Lock P (2012). Prognostic significance of Tks5 expression in gliomas. *J Clin Neurosci* **19**(3), 436–442.
- [16] Baskar R, Lee K, Yeo R, and Yeoh K-W (2012). Cancer and radiation therapy: current advances and future directions. *Int J Med Sci* **9**(3), 193–199.
- [17] Araya J, Maruyama M, Sassa K, Fujita T, Hayashi R, Matsui S, Kashii T, Yamashita N, Sugiyama E, and Kobayashi M (2001). Ionizing radiation enhances matrix metalloproteinase-2 production in human lung epithelial cells. *Am J Physiol Lung Cell Mol Physiol* **280**(1), L30–L38.
- [18] Qian L-W, Mizumoto K, Urashima T, Nagai E, Maehara N, Sato N, Nakajima M, and Tanaka M (2002). Radiation-induced increase in invasive potential of human pancreatic cancer cells and its blockade by a matrix metalloproteinase inhibitor, CGS27023. *Clin Cancer Res* **8**(4), 1223–1227.
- [19] Zhao W, O'Malley Y, Wei S, and Robbins MEC (2000). Irradiation of rat tubule epithelial cells alters the expression of gene products associated with the synthesis and degradation of extracellular matrix. *Int J Radiat Biol* **76**(3), 391–402.
- [20] Park C-M, Park M-J, Kwak H-J, Lee H-C, Kim M-S, Lee S-H, Park I-C, Rhee C, and Hong S-I (2006). Ionizing radiation enhances matrix metalloproteinase-2 secretion and invasion of glioma cells through Src/epidermal growth factor receptor-mediated p38/Akt and phosphatidylinositol 3-kinase/Akt signaling pathways. *Cancer Res* **66**(17), 8511–8519.
- [21] Pei J, Park I-H, Ryu H-H, Li S-Y, Li C-H, Lim S-H, Wen M, Jang W-Y, and Jung S (2015). Sublethal dose of irradiation enhances invasion of malignant glioma cells through p53-MMP 2 pathway in U87MG mouse brain tumor model. *Radiat Oncol* **10**(1), 164.
- [22] Sawaya R, Tofoni P, Mohanam S, Ali Oosman F, Liotta L, Stetler Stevenson W, and Rao J (1994). Induction of tissue-type plasminogen activator and 72-kDa type-IV collagenase by ionizing radiation in rat astrocytes. *Int J Cancer* **56**(2), 214–218.
- [23] Badiga A, Chetty C, Kesanakurti D, Are D, Gujrati M, Klopfenstein J, Dinh D, Rao J, and Lesniak M (2011). MMP-2 siRNA inhibits radiation-enhanced invasiveness in glioma cells. *PLoS One* **6**(6)e20614.
- [24] Cordes N, Hansmeier B, Beinke C, Meineke V, and van Beuningen D (2003). Irradiation differentially affects substratum-dependent survival, adhesion, and invasion of glioblastoma cell lines. *Br J Cancer* **89**(11), 2122–2132.
- [25] Hegedus B, Zach J, Czirok A, Lovey J, and Vicssek T (2004). Irradiation and Taxol treatment result in non-monotonous, dose-dependent changes in the motility of glioblastoma cells. *J Neuro-Oncol* **67**(1–2), 147–157.
- [26] Trog D, Fountoulakis M, Friedlein A, and Golubnitschaja O (2006). Is current therapy of malignant gliomas beneficial for patients? Proteomics evidence of shifts in glioma cells expression patterns under clinically relevant treatment conditions. *Proteomics* **6**(9), 2924–2930.
- [27] Trog D, Yeghiazaryan K, Fountoulakis M, Friedlein A, Moenkemann H, Haertel N, Schueller H, Breipohl W, Schild H, and Leppert D, et al (2006). Pro-invasive gene regulating effect of irradiation and combined temozolomide-radiation treatment on surviving human malignant glioma cells. *Eur J Pharmacol* **542**(1), 8–15.
- [28] Wild-Bode C, Weller M, Rimmer A, Dichgans J, and Wick W (2001). Sublethal irradiation promotes migration and invasiveness of glioma cells. Implications for radiotherapy of human glioblastoma. **61**(6), 2744–2750.
- [29] Kosztyla R, Chan E, Hsu F, Wilson D, Ma R, Cheung A, Zhang S, Moiseenko V, Benard F, and Nichol A (2013). High-grade glioma radiation therapy target volumes and patterns of failure obtained from magnetic resonance imaging and 18F-FDOPA positron emission tomography delineations from multiple observers. *Int J Radiat Oncol Biol Phys* **87**(5), 1100–1106.
- [30] Mao L, Whitehead CA, Paradiso L, Kaye AH, Morokoff AP, Luwor RB, and Stylli SS (2017). Enhancement of invadopodia activity in glioma cells by sublethal doses of irradiation and temozolomide. *J Neurosurg*, 1–13.
- [31] Mullard A (2014). 2013 FDA drug approvals. *Nat Rev Drug Discov* **13**(2), 85–89.
- [32] Chong CR and Sullivan Jr DJ (2007). New uses for old drugs. *Nature* **448** (7154), 645–646.
- [33] Stylli SS, I STT, Verhagen AM, Xu SS, Pass I, Courtneidge SA, and Lock P (2009). Nck adaptor proteins link Tks5 to invadopodia actin regulation and ECM degradation. *J Cell Sci* **122**(15), 2727–2740.
- [34] Artym V, Zhang Y, Seillier Moiseiwitsch F, Yamada K, and Mueller S (2006). Dynamic interactions of cortactin and membrane type 1 matrix metalloproteinase at invadopodia: defining the stages of invadopodia formation and function. *Cancer Res* **66**(6), 3034–3043.
- [35] Jacob A, Linklater E, Bayless BA, Lyons T, and Prekeris R (2016). The role and regulation of Rab40b-Tks5 complex during invadopodia formation and cancer cell invasion. *J Cell Sci* **129**(23), 4341–4353.
- [36] Clark E, Whigham A, Yarbrough W, and Weaver A (2007). Cortactin is an essential regulator of matrix metalloproteinase secretion and extracellular matrix degradation in invadopodia. *Cancer Res* **67**(9), 4227–4235.
- [37] Mader CC, Oser M, Magalhaes MAO, Bravo-Cordero JJ, Condeelis J, Koleske AJ, and Gil-Henn H (2011). An EGFR-Src-Arg-cortactin pathway mediates functional maturation of invadopodia and breast cancer cell invasion. *Cancer Res* **71**(5), 1730–1741.
- [38] Ayala I, Baldassarre M, Giacchetti G, Caldieri G, Tetè S, Luini A, and Buccione R (2008). Multiple regulatory inputs converge on cortactin to control invadopodia biogenesis and extracellular matrix degradation. *J Cell Sci* **121**(3), 369–378.
- [39] Rhodes DR, Kalyana-Sundaram S, Mahavisno V, Varambally R, Yu J, Briggs BB, Barrette TR, Anstet MJ, Kincaid-Beal C, and Kulkarni P, et al (2007). Oncomine 3.0: genes, pathways, and networks in a collection of 18,000 cancer gene expression profiles. *Neoplasia* **9**(2), 166–180.
- [40] Stupp R, Mason W, Van Den Bent M, Weller M, Fisher B, Taphoorn M, Brandes A, Cairncross G, Lacombe D, and Mirimanoff R (2004). Concomitant and adjuvant temozolomide (TMZ) and radiotherapy (RT) for newly diagnosed glioblastoma multiforme (GBM). Conclusive results of a randomized phase III trial by the EORTC Brain & RT Groups and NCIC Clinical Trials Group. *J Clin Oncol* **22**(14_Suppl), 2.
- [41] Imperato J, Paleologos N, and Vick N (1990). Effects of treatment on long-term survivors with malignant astrocytomas. *Ann Neurol* **28**(6), 818–822.
- [42] Coopman PJ, Do MT, Thompson EW, and Mueller SC (1998). Phagocytosis of cross-linked gelatin matrix by human breast carcinoma cells correlates with their invasive capacity. *Clin Cancer Res* **4**(2), 507–515.
- [43] Gligorijevic B, Wyckoff J, Yamaguchi H, Wang Y, Roussos E, and Condeelis J (2012). N-WASP-mediated invadopodium formation is involved in intravasation and lung metastasis of mammary tumors. *J Cell Sci* **125**(3), 724–734.
- [44] Hayes KE, Walk EL, Ammer AG, Kelley LC, Martin KH, and Weed SA (2013). Ablens kinases negatively regulate invadopodia function and invasion in head and neck squamous cell carcinoma by inhibiting an HB-EGF autocrine loop. *Oncogene* **32**(40), 4766–4777.
- [45] Monsky WL, Lin CY, Aoyama A, Kelly T, Akiyama SK, Mueller SC, and Chen WT (1994). A potential marker protease of invasiveness, seprase, is localized on invadopodia of human malignant melanoma cells. *Cancer Res* **54**(21), 5702–5710.

- [46] Schoumacher M, Goldman R, Louvard D, and Vignjevic D (2010). Actin, microtubules, and vimentin intermediate filaments cooperate for elongation of invadopodia. *J Cell Biol* **189**(3), 541–556.
- [47] Sutoh M, Hashimoto Y, Yoneyama T, Yamamoto H, Hatakeyama S, Koie T, Okamoto A, Yamaya K, Saitoh H, and Funyu T, et al (2010). Invadopodia formation by bladder tumor cells. *Oncol Res* **19**(2), 85–92.
- [48] Takkanen M, Hukkanen M, Liljeström M, Grenman R, and Virtanen I (2010). Podosome-like structures of non-invasive carcinoma cells are replaced in epithelial-mesenchymal transition by actin comet-embedded invadopodia. *J Cell Mol Med* **14**(6b), 1569–1593.
- [49] Yamaguchi H (2012). Pathological roles of invadopodia in cancer invasion and metastasis. *Eur J Cell Biol* **91**(11–12), 902–907.
- [50] Yamamoto H, Sutoh M, Hatakeyama S, Hashimoto Y, Yoneyama T, Koie T, Saitoh H, Yamaya K, Funyu T, and Nakamura T, et al (2011). Requirement for FBP17 in invadopodia formation by invasive bladder tumor cells. *J Urol* **185**(5), 1930–1938.
- [51] Steinle M, Palme D, Misovic M, Rudner J, Dittmann K, Lukowski R, Ruth P, and Huber S (2011). Ionizing radiation induces migration of glioblastoma cells by activating BK K(+) channels. *Radiother Oncol* **101**(1), 122–126.
- [52] Mentlein R, Hattermann K, and Held-Feindt J (2012). Lost in disruption: role of proteases in glioma invasion and progression. *Biochim Biophys Acta Rev Cancer* **1825**(2), 178–185.
- [53] Yang C-PH and Horwitz SB (2017). Taxol®: the first microtubule stabilizing agent. *Int J Mol Sci* **18**(8), 1–11 1733.
- [54] Barletta G, Genova C, Rijavec E, Burrafato G, Biello F, Sini C, Dal Bello MG, Coco S, Truini A, and Vanni I (2014). Oral vinorelbine in the treatment of non-small-cell lung cancer. *Expert Opin Pharmacother* **15**(11), 1585–1599.
- [55] Cvitkovic E and Izzo J (1992). The current and future place of vinorelbine in cancer therapy. *Drugs* **44**(4), 36–45.
- [56] Minchinton AI and Tannock IF (2006). Drug penetration in solid tumours. *Nat Rev Cancer* **6**(8), 583–592.
- [57] Samala R, Thorsheim HR, Goda S, Taskar K, Gril B, Steeg PS, and Smith QR (2016). Vinorelbine delivery and efficacy in the MDA-MB-231BR preclinical model of brain metastases of breast cancer. *Pharm Res* **33**(12), 2904–2919.
- [58] Gregory RK and Smith IE (2000). Vinorelbine—a clinical review. *Br J Cancer* **82**(12), 1907–1913.
- [59] Horwitz SB (1994). Taxol (paclitaxel): mechanisms of action. *Ann Oncol* **5** (Suppl. 6), S3–S6.
- [60] Dumontet C and Sikic BI (1999). Mechanisms of action of and resistance to antitubulin agents: microtubule dynamics, drug transport, and cell death. *J Clin Oncol* **17**(3), 1061–1070.
- [61] Ngan VK, Bellman K, Panda D, Hill BT, Jordan MA, and Wilson L (2000). Novel actions of the antitumor drugs vinflunine and vinorelbine on microtubules. *Cancer Res* **60**(18), 5045–5051.
- [62] Ashamalla H, Zaki B, Mokhtar B, Lewis L, Lavaf A, Nasr H, Colella F, Dosik D, Krishnamurthy M, and Saad N, et al (2007). Fractionated stereotactic radiotherapy boost and weekly paclitaxel in malignant gliomas clinical and pharmacokinetics results. *Technol Cancer Res Treat* **6**(3), 169–176.
- [63] Julka PK, Awasthy BS, Rath GK, Agarwal S, Varna T, Mahapatra AK, and Singh R (2000). A study of concurrent radiochemotherapy with paclitaxel in glioblastoma multiforme. *Australas Radiol* **44**(1), 84–87.
- [64] Jeyapalan S, Boxerman J, Donahue J, Goldman M, Kinsella T, Dipetrillo T, Evans D, Elinzano H, Constantinou M, and Stopa E, et al (2014). Paclitaxel poliglumex, temozolomide, and radiation for newly diagnosed high-grade glioma: a Brown University Oncology Group Study. *Am J Clin Oncol* **37**(5), 444–449.
- [65] Biassoni V, Casanova M, Spreafico F, Gandola L, and Massimino M (2006). A case of relapsing glioblastoma multiforme responding to vinorelbine. *J Neuro-Oncol* **80**(2), 195–201.